iJRASET
International Journal For Research in Applied Science and Engineering Technology



INTERNATIONAL JOURNAL FOR RESEARCH

IN APPLIED SCIENCE & ENGINEERING TECHNOLOGY

Volume: 13 **Issue:** IX **Month of publication:** September 2025

DOI: https://doi.org/10.22214/ijraset.2025.73992

www.ijraset.com

Call: 08813907089 | E-mail ID: ijraset@gmail.com

International Journal for Research in Applied Science & Engineering Technology (IJRASET)
ISSN: 2321-9653; IC Value: 45.98; SJ Impact Factor: 7.538
Volume 13 Issue IX Sep 2025- Available at www.ijraset.com

A Semi Analytical Method for Dynamic Analysis of Beam Resting on Inertial Soil

Revathy Mohan
Independent Structural Engineer, Kerala, India

Abstract: ***Accurate dynamic analysis of beams supported on soil is essential for the safe and economical design of vibration-resistant and earthquake-resistant structures. Earlier contributions, such as the semi-analytical framework developed by Guenfoud, Bosakov, and Laefer (2009), provided reliable predictions for beams on elastic half-spaces with inertial properties. However, these formulations are mathematically intensive and often difficult to apply directly in engineering practice. Conventional soil models, including Winkler's subgrade reaction method and continuum-based elastic models, either oversimplify soil behaviour or involve complex derivations, further limiting their practical utility. The present study introduces a modified version of the semi-analytical method for beams resting on an elastic half-space with inertial properties, reformulated to reduce mathematical complexity without compromising accuracy. The approach incorporates soil inertia effects while enabling more straightforward evaluation of displacements under vertical loading. To illustrate its effectiveness, the dynamic response of a beam measuring 10 m in length, 1 m in width, and 0.5 m in depth is investigated. The corresponding Eigenfrequencies and natural shapes of the beam are determined, and the results show close agreement with those obtained from established analytical methods. This refinement not only simplifies computational effort but also makes the analysis more accessible for engineering applications. The method thus provides a practical and reliable tool for studying beam–soil interaction dynamics, with direct relevance for the design of safer and more cost-effective structural systems.***

Keywords: ***Response function, Inertial soil effects, Flexural element, Natural frequencies, Mode shapes, Vibration response, Transient response,***

I. INTRODUCTION

A *fundamental solution* represents an analytical expression describing how a solid responds at any location due to a static or dynamic point load applied elsewhere. Such formulations, often referred to as *influence functions*, serve as essential building blocks for developing more complex solutions. During the 19th and early 20th centuries, mathematicians and engineering scientists laid the theoretical foundation and introduced these solutions, commonly known as *Green's functions*, which enabled significant progress in the field of soil–structure interaction (SSI).

Several techniques exist for analysing beams supported on elastic soils. Among them, two are particularly significant: the *subgrade reaction method* and the *elastic continuum (modulus of elasticity) approach*. The Winkler subgrade model idealizes the soil as a series of independent springs, where deflection at a point depends solely on the local pressure and is unaffected by adjacent loads. In this sense, the beam is considered to rest on discrete, infinitely long springs defined by a subgrade modulus. By contrast, the elastic continuum model accounts for the influence of neighbouring soil regions through Boussinesq's load–displacement relation for a homogeneous, isotropic half-space. Here, the soil is represented using material parameters such as elastic modulus and Poisson's ratio. While this model more accurately reflects soil behaviour, solving its governing differential equations can be computationally demanding, often requiring approximate solution strategies. Over the years, various methods have been developed for computing the *dynamic response* of soil–foundation systems, which can be broadly grouped into six categories:

1) Simplified procedures – Based on physical approximations and fundamental principles of dynamics and wave propagation. Solutions are often presented in the form of design charts and graphs, making them easily usable by practicing engineers, especially for embedded foundations and piles.

2) Semi-analytical formulations – Applied to surface foundations of varying shapes and stiffness. The contact surface is discretized, dynamic impedance functions are determined for unit loads, and complete solutions are constructed using Fast Fourier Transform (FFT) schemes.

3) Analytical methods – Developed under the assumption of no shear or normal tractions at the soil–foundation interface during vertical or rocking motion. These methods rely on solving integral transforms of dual wave equations for layered systems or half-spaces.

©IJRASET: All Rights are Reserved | SJ Impact Factor 7.538 | ISRA Journal Impact Factor 7.894 |

4) Dynamic finite element models – Used to capture responses of foundations in multi-layered soils or in the presence of inhomogeneities. Unlike static FEM, special boundary conditions such as *absorbing* or *viscous* boundaries are introduced to prevent spurious wave reflections and to simulate far-field damping.

5) Boundary element methods – Semi-analytical techniques that transform the problem into a system of algebraic equations relating nodal forces and displacements, while satisfying reciprocity and radiation conditions.

6) Experimental approaches – Laboratory and field studies have been widely conducted to evaluate soil dynamics. These tests not only provide direct insight into soil–foundation response but also validate theoretical and numerical predictions. They are applicable for both surface and embedded foundations and often require less analytical complexity.

In this study, a semi-analytical procedure has been employed to derive the required structural response, combining computational efficiency with the ability to account for soil inertia effects.

II. PROBLEM APPROACH

In this formulation, the natural frequencies, vibration modes, and load-induced response of a beam supported by an elastic medium with inertia are evaluated on the basis of Lamb's problem. The procedure builds upon the method of Zhemochkin and Sinitsyn [17], where the beam is discretized into uniform elements of length c_i width b_i. This line of development was further advanced by Guenfoud et al. [3].

In the present study, the supporting soil is modeled as a homogeneous, isotropic elastic half-space that includes inertial effects. For simplicity, surface curvature, damping characteristics, and friction within the beam–soil contact region are not considered. The beam itself, with total mass *m* and flexural rigidity EI, is assumed to rest directly on the half-space and subjected to external vertical excitation (Fig. 1).

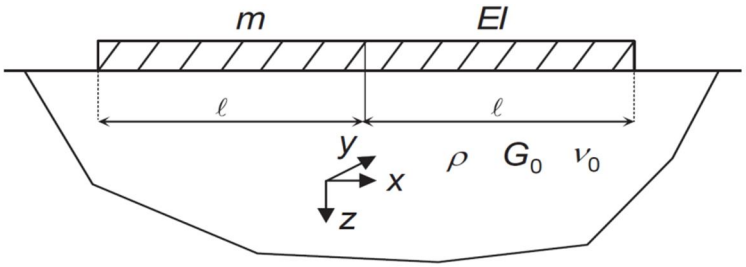


Fig.1. The beam with mass m and flexural rigidity EI rest directly on the half-space and subjected to external vertical excitation

Instead of assuming continuous beam–soil contact, the model idealizes the interaction as discontinuous, with each element connected to the half-space through a rigid vertical link at its midpoint.

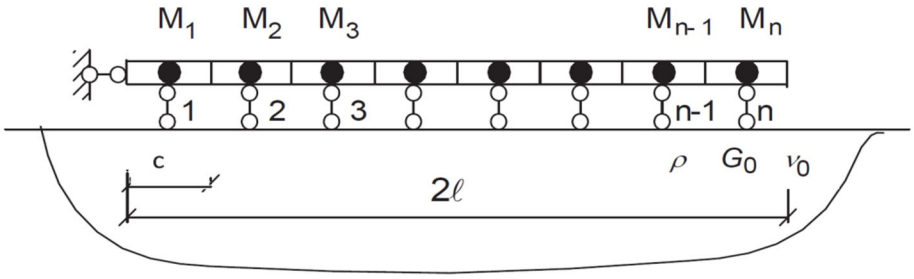


Fig.2. The continuous contact surface of beam is approximated by a series of discrete rigid vertical connectors, each positioned at the centre of the corresponding beam element.

©IJRASET: All Rights are Reserved | SJ Impact Factor 7.538 | ISRA Journal Impact Factor 7.894 |

A detailed force spring rotation diagram of fig.(2) is given in figure (3)

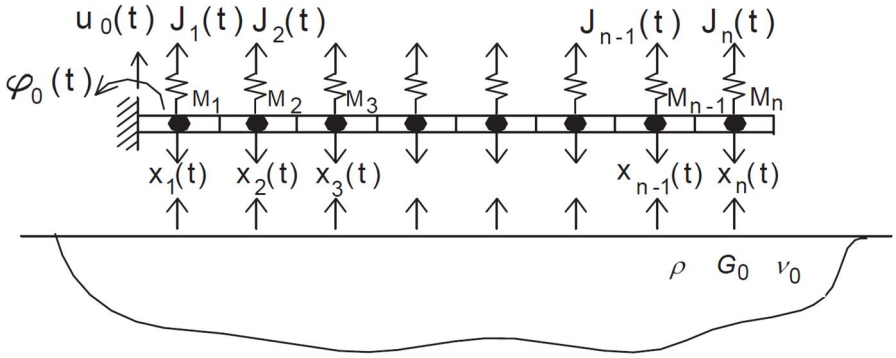


Fig. 3. Discretized representation of the beam–half-space system illustrating the applied forces and unknown parameters of the indeterminate model.

The normal equations according to Zhemochkin and Sinitsyn [17] take the form of Eq. (1)

$$\begin{aligned}
&\sum_{j=1}^{n}(v_{ij}+y_{ij})X_j(t)-\sum_{j=1}^{n}y_{ij}J_j(t)+\lambda_i\Phi_0(t)+u_0(t)+\Delta_{ip}=0\ ;\ i=1,\ldots,n\\
&\sum_{j=1}^{n}[(X_j(t)-J_j(t)]\lambda_j=I_y\ddot{\Phi}_0(t)\\
&\sum_{j=1}^{n}[(X_j(t)-J_j(t)]=m\ddot{u}_0(t)
\end{aligned}\qquad (1)$$

In this equation the unknowns are $X_i(t)$, $\Phi_0(t)$, $u_0(t)$

Where,

$X_i(t)$ - liaison efforts ; $\Phi_0(t)$ - angle of rotation ; $u_0(t)$ - vertical displacement v_{ij} - Green's function defining the displacement of the surface of a half-space at the point i due to the unitary force $R_j = 1$ applied at the point j of the same surface ; $\Delta_i P$ - a function characterizing deflection of the beam at the point i due to external loads ; Pp - external load applied in the point p of the beam : $J_k(t)$ - inertia forces.

The free vibrations of the beam are supposed to be in harmonic form, which can be expressed as Eq. (2)

$$\begin{aligned}
&X_k(t)=X_k e^{i\omega t}\\
&\Phi_0(t)=\Phi_0 e^{i\omega t}\ ;\\
&u_0(t)=u_0 e^{i\omega t}\ ;\\
&J_k(t)=J_k e^{i\omega t}
\end{aligned}\qquad (2)$$

Where X_k, ϕ_0, u_0, J_k are amplitude values of $X_k(t)$, $\Phi_0(t)$, $u_0(t)$, and $J_k(t)$, respectively. By substituting these values in eq. (1) we will get the following equation

$$\begin{aligned}
&\sum_{j=1}^{n}(v_{ij}+y_{ij})X_j-\sum_{j=1}^{n}y_{ij}J_j+\lambda_i\Phi_0+u_0=0;\quad i=1,\ldots,n\\
&\sum_{j=1}^{n}[(X_j-J_j]\lambda_j=-\omega^2 I_y\Phi_0\\
&\sum_{j=1}^{n}[(X_j-J_j]=-\omega^2 m u_0
\end{aligned}\qquad (3)$$

A. Green's function for the vertical displacements

Green's function defining the vertical displacements of a half- space surface with inertial properties due to the action of external harmonic load $Pe^{i\omega t}$ is given by

$$V=\frac{Pe^{i\omega t}}{2\pi G_0}[I_\xi+i\pi\chi K J_0(\chi r)] \qquad (4)$$

$$I_\xi=\int_0^\infty \frac{k^2\xi\alpha}{F(\xi)}J_0(\xi r)d\xi \qquad (5)$$

$$K=\frac{2k^2\alpha_1(2\chi^2-k^2)^2}{-F'(\chi)f(\chi)} \qquad (6)$$

©IJRASET: All Rights are Reserved | SJ Impact Factor 7.538 | ISRA Journal Impact Factor 7.894 |

Where

$F(\xi)=(2\xi^2-k^2)^2-4\xi^2\,\alpha\beta$

$f(\xi)=(2\xi^2-k^2)^2+4\xi^2\,\alpha\beta$

χ is the root of equation $f(\xi)=0$

According to Guenfoud et al. [3] after simplifications, Eq. (4) becomes

$$\mathbf{v}=\frac{-kPe^{i\omega t}}{2\pi G0}\{(I_{21}+I_3)+i[(I_1+I_{22})\frac{\pi\chi KJ_0(\chi r)}{k}]\} \quad (7)$$

In which

$$I_1 = \int_0^{1/2}\Phi_1(\theta)j_0(k\theta r)d\theta \quad (8)$$

$$I_{21} = \int_0^{1/2}\Phi_2(\theta)j_0(k\theta r)d\theta \quad (9)$$

$$I_{22} = \int_0^{1/2}\Phi_3(\theta)j_0(k\theta r)d\theta \quad (10)$$

$$I_3 = \int_0^{1/2}\Phi_4(\theta)j_0(k\theta r)d\theta \quad (11)$$

Where

$k\theta=\xi$; $\theta=\sqrt{(1-2v_0)/2(1-v_0)}$

$$\Phi_1(\theta)=\frac{\theta\sqrt{0.25-\theta^2}}{(1-2\theta^2)^2+4\theta^2\sqrt{0.25-\theta^2}\times\sqrt{1-\theta^2}} \qquad 0\le\theta\le 0.5$$

$$\Phi_2(\theta)=\frac{-\theta(1-2\theta^2)^2\sqrt{\theta^2-0.25}}{-4\theta^4(\theta^2-1)+[-1+8(\theta^2+3\theta^4+2\theta^6)]} \qquad 0.5\le\theta\le 1$$

$$\Phi_3(\theta)=\frac{-4\theta^3(\theta^2-0.25)\sqrt{1-\theta^2}}{-4\theta^4(\theta^2-1)+[-1+8(\theta^2+3\theta^4+2\theta^6)]} \qquad 0.5\le\theta\le 1$$

$$\Phi_4(\theta)=\frac{-\theta\sqrt{\theta^2-0.25}}{4\theta^2\sqrt{\theta^2-1}\times\sqrt{\theta^2-0.25}-(1-2\theta^2)^2} \qquad 1\le\theta\le\infty$$

The values of I_1, I_{21}, I_{22} and I_3 are determined by using Gaussian quadrature with modification in a way similar to that used by Guenfoud et al. [3].

Considering the external load, $Pe^{i\omega t}=P\cos(\omega t)$ and taking into account only the real part of Eq.(7) then the value of displacement becomes equal to Eq. (12)

$$\mathbf{v}=(I_{21}+I_3) \quad (12)$$

For unit external load equation (12) can be written as

$$\mathbf{v}=\frac{-k\cos(\omega t)}{2\pi G_0}(I_{21}+I_3) \quad (13)$$

For application of the proposed approach, Eq. (5) should be integrated over the area of the loaded element with dimensions b and c Therefore, the variable r becomes;

$r=\sqrt{x^2+y^2}$ then equation (13) becomes

$$V=\frac{-k\cos(\omega t)}{2bc\pi G_0}\int_{X_1}^{X_2}\int_{Y_1}^{Y_2}[\,I_{21}(\sqrt{x^2+y^2})+I_{21}(\sqrt{x^2+y^2})\,]dxdy \quad (14)$$

Here the expression is divided into the magnitude bc, as loading is considered uniformly distributed across a rectangular element with dimension b and c

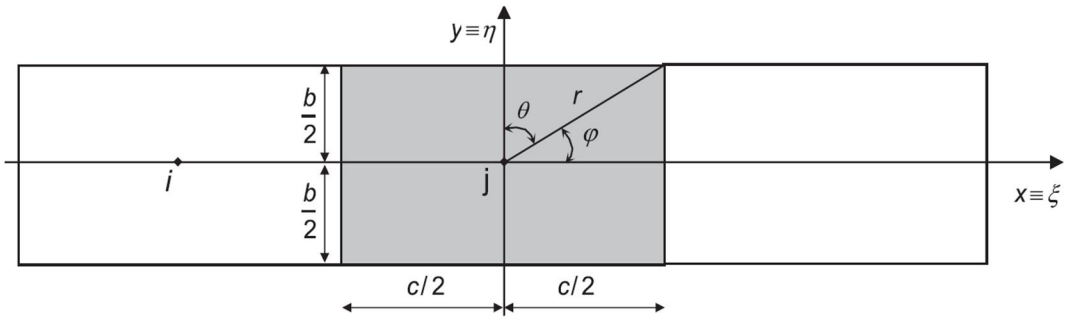


Fig.4. Geometry of the loaded element showing the area over which the integration should occur

©IJRASET: All Rights are Reserved | SJ Impact Factor 7.538 | ISRA Journal Impact Factor 7.894 |

In this case as r→ 0, the point i coincide with the point j and thus above equation is integrated over the area of the loaded element assuming a uniformly distributed load. This is shown in following equation

$$v = \frac{-k\cos(\omega)t}{2bc\pi G_0}\int_{-c/2}^{c/2}\int_{-b/2}^{-b/2}\left[I_{21}\left(\sqrt{(x-\xi)^2+\eta^2}\right)+I_3\left(\sqrt{(x-\xi)^2+\eta^2}\right)\right]d\eta d\xi \qquad (15)$$

Certain portions of the integrals I_{21} and I_3 in formula can be evaluated directly, whereas the remaining terms are too complex for straightforward computation. To address this difficulty, the method proposed by Johnson [18] is employed, where the Cartesian coordinate system is transformed into polar coordinates. This transformation enables the calculation of displacements at a point located diagonally with respect to the origin (Fig. 4). Incorporating Johnson's procedure modifies Eq. (15) into the form presented as Eq. (16).

$$V=\frac{-2k\cos(\omega t)}{bc\pi G_0}\left\{\int_0^{\arctan\left(\frac{c}{b}\right)}\int_0^{\frac{b}{2}\cos\theta}\left[I_{21}\left(\sqrt{(x-\xi)^2+\eta^2}+I_3\left(\sqrt{(x-\xi)^2+\eta^2}\right)\right]\right\}rdrd\Phi$$

$$+\int_0^{\arctan\left(\frac{c}{b}\right)}\int_0^{\frac{b}{2}\cos\theta}\left[I_{21}\left(\sqrt{(x-\xi)^2+\eta^2}\right)+I_3\left(\sqrt{(x-\xi)^2+\eta^2}\right)\right]\}rdrd\Phi \qquad (16)$$

In this case, r≠0 we divides the loaded element into 16 smaller elements as in figure (5)

Consequently, the displacement of the half-space surface accounting for inertial effects can be represented by equation (17).

$$V=\frac{-k\cos(\omega t)}{2\pi G}\left\{\frac{1}{16}\sum_{n=1}^{16}\left[I_{21}\left(\sqrt{(x-\xi_n)^2+\eta_n{}^2}\right)+I_3\left(\sqrt{(x-\xi_n)^2+\eta_n{}^2}\right)\right]\right\} \qquad (17)$$

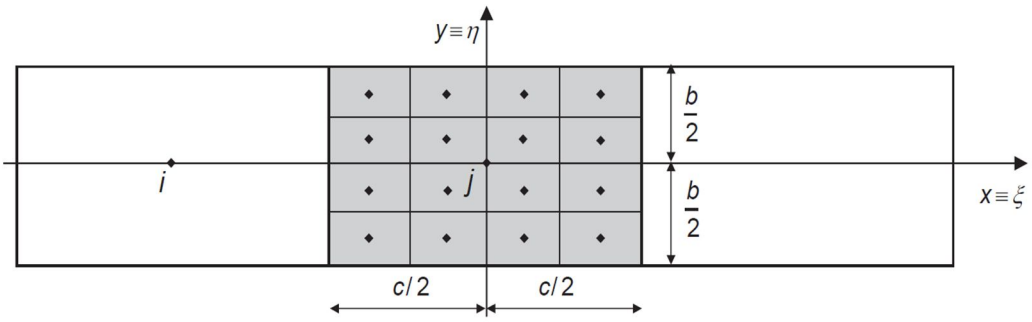
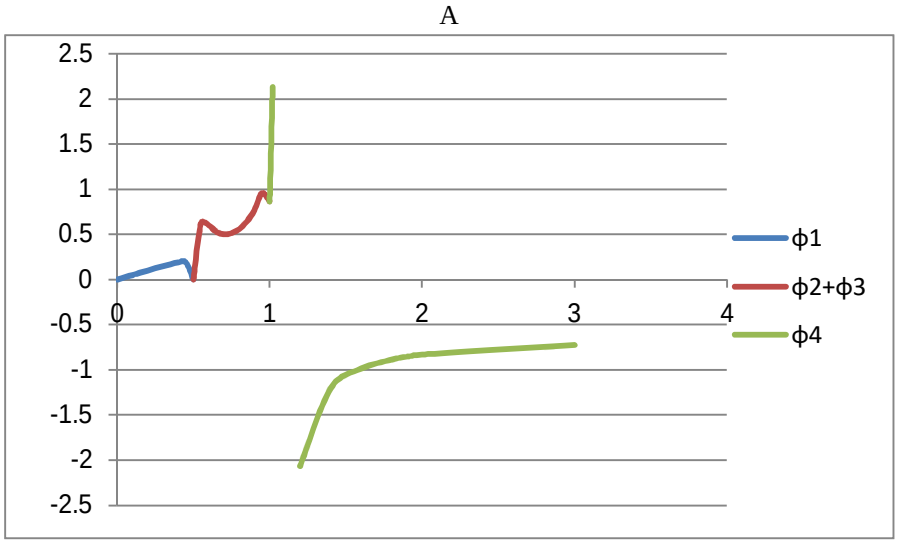


Fig.5.The loaded element is divided into smaller elements

B. Validation of present approach



©IJRASET: All Rights are Reserved | SJ Impact Factor 7.538 | ISRA Journal Impact Factor 7.894 |

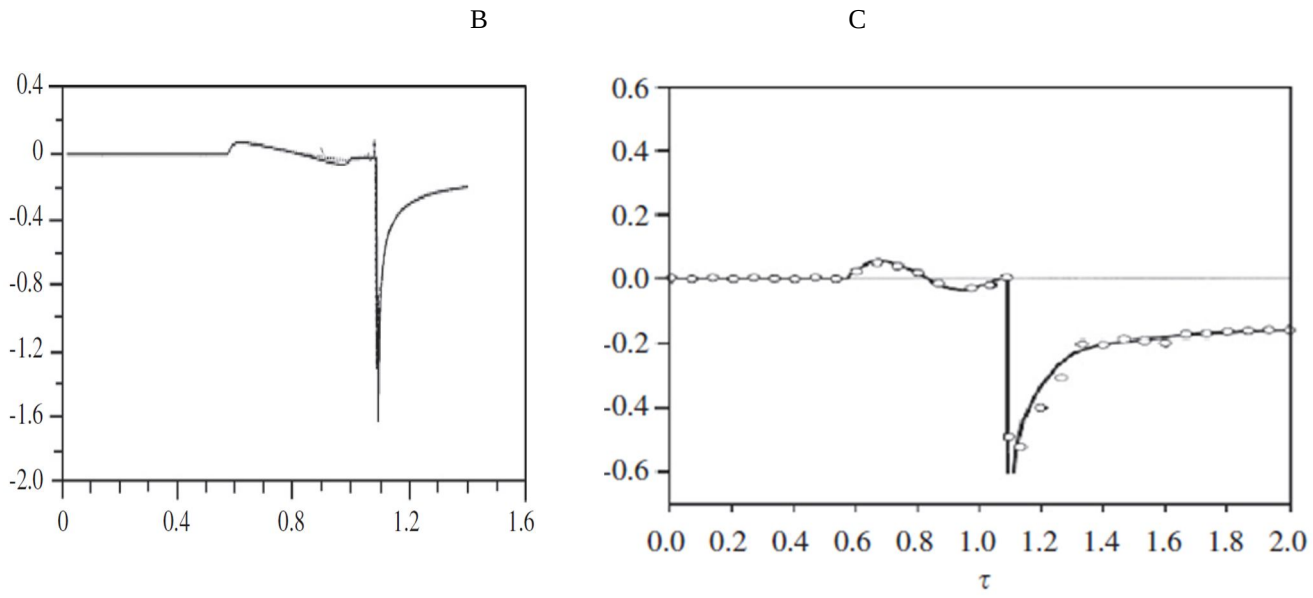


Fig. 6. Comparison of results :(A) by present approach, (B) Georgiadis [19].and (C) Zeng [20]

Figure 6 illustrates how displacements on the half-space surface vary with time at an arbitrary point. It can be observed that both radial and vertical displacements approach infinity when the Rayleigh wave arrives, corresponding to a specific value of the dimensionless time parameter τ. From the present solution, this critical point occurs at $\theta=\chi=1.07236$, where the singularity appears. This value coincides with those reported in the literature [19, 20], thereby supporting the validity of the current approach.

The graphical plots of functions I_1, I_{21}, I_{22} and I_3 are presented below. The results show close agreement with the findings of Guenfoud et al. [3] (see Fig. 11).

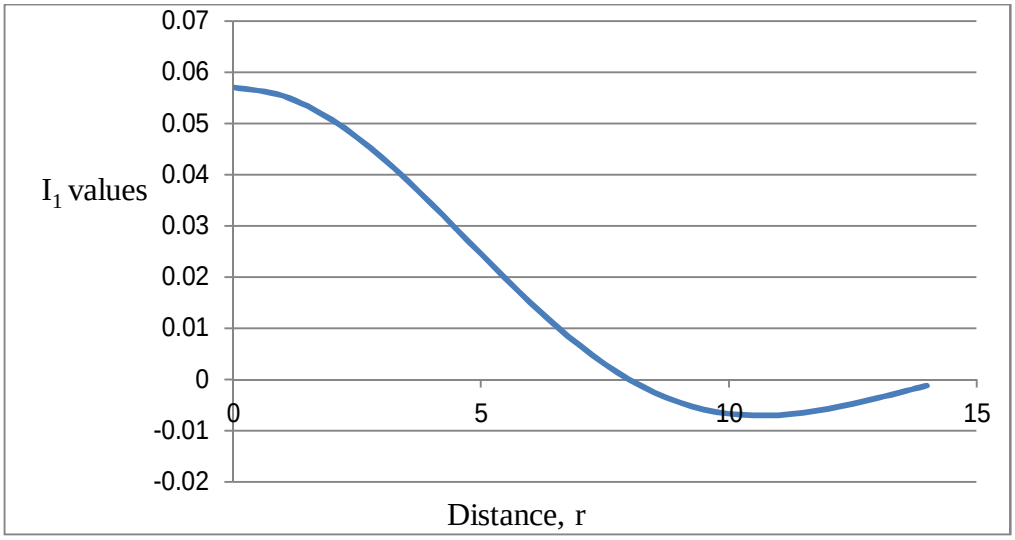


Fig .7. Graphic representation of I_1

©IJRASET: All Rights are Reserved | SJ Impact Factor 7.538 | ISRA Journal Impact Factor 7.894 |

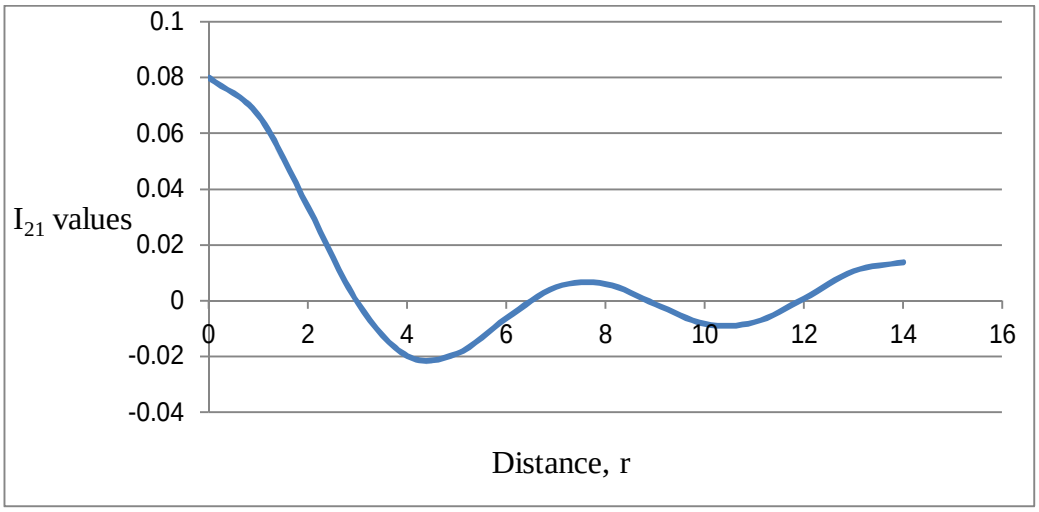


Fig 8. Graphic representation of I_{21}

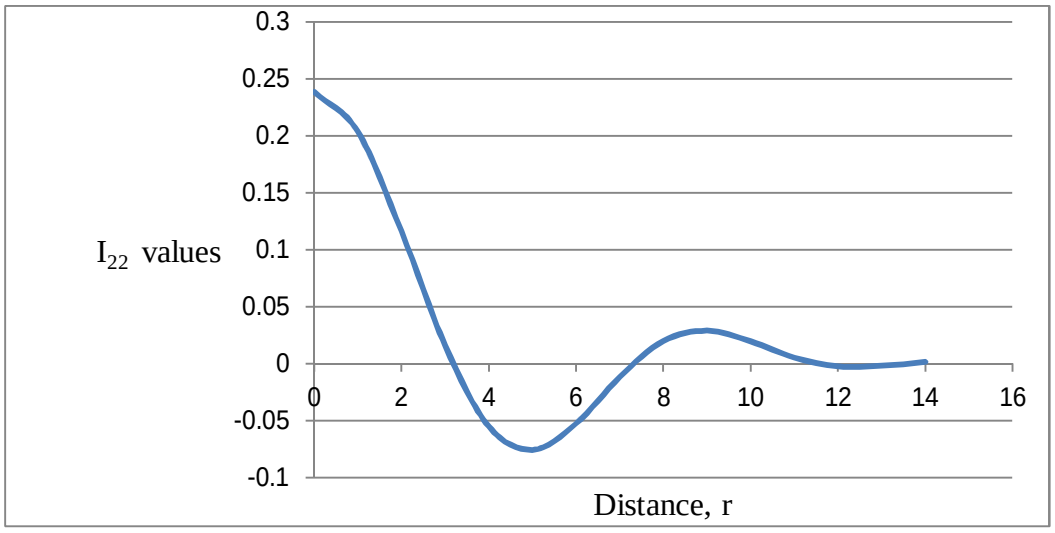


Fig .9. Graphic representation of I_{22}

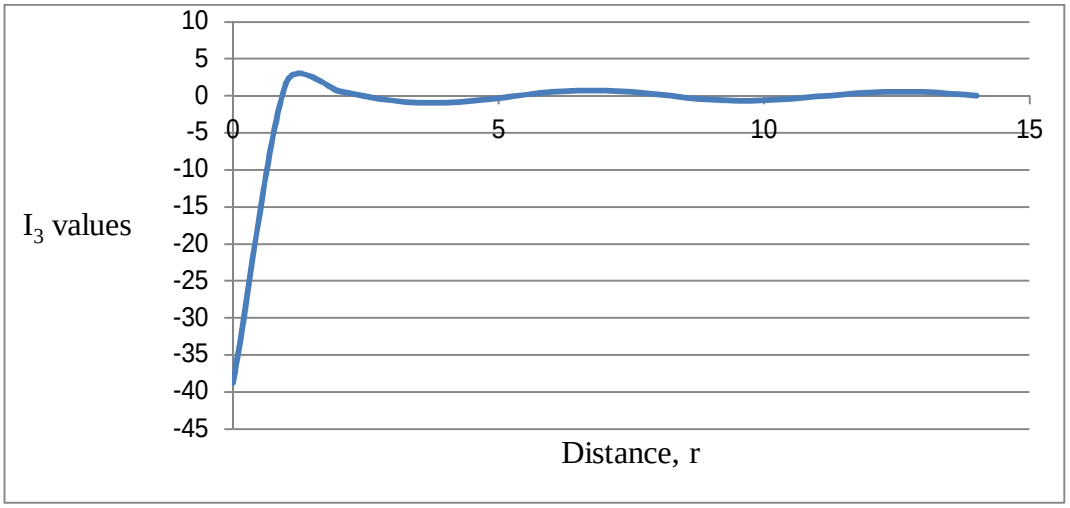


Fig .10. Graphic representation of I_3

©IJRASET: All Rights are Reserved | SJ Impact Factor 7.538 | ISRA Journal Impact Factor 7.894 |

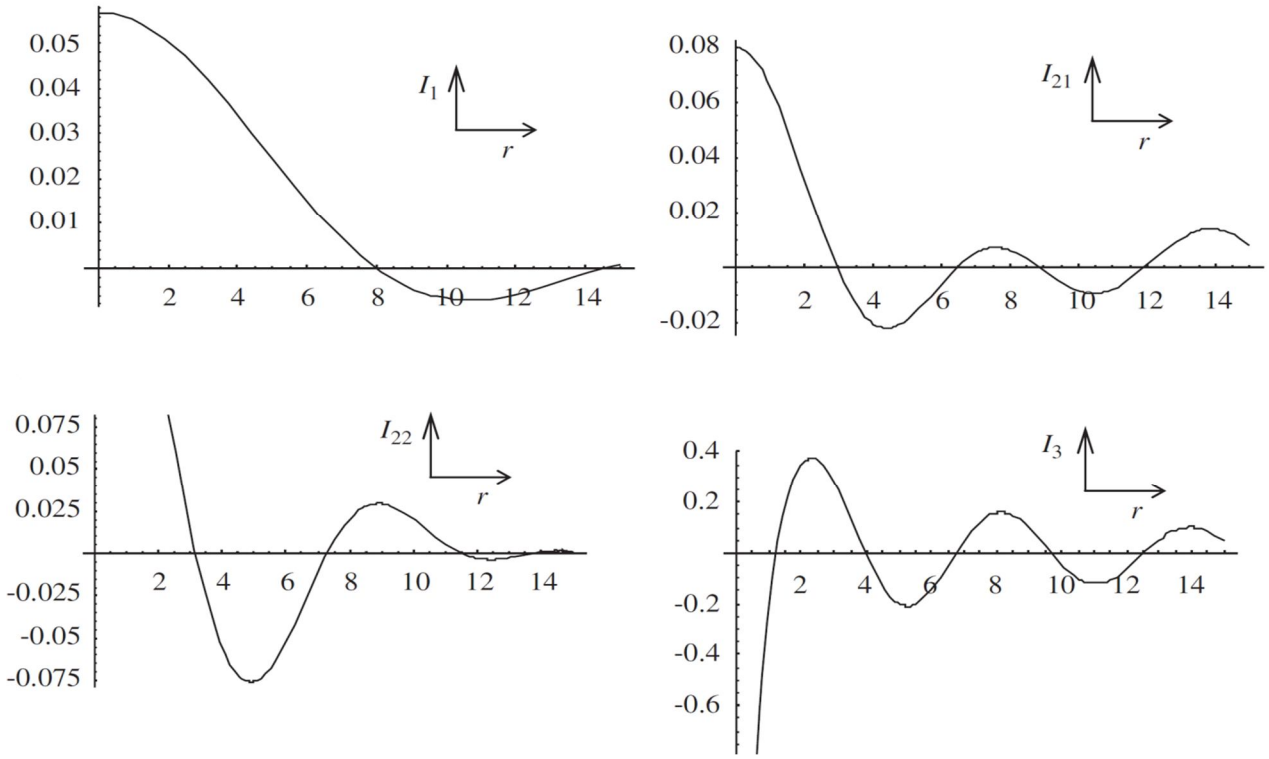


Fig .11. Graphic representation of I_1, I_{21}, I_{22} and I_3 obtained by Guenfoud et.al [3]

According to Guenfoud et al.[4] the value of $I_{21}+I_3$ can be determined approximately by using equation (18)

$I_{21}+I_3$= -0.06387/kr+0.13+0.14ln(1.07236k)+0.14ln(r)+ 0.15278kr + [0.15k^2- 0.04k^2ln(1.07236k) - 0.04k^2 ln(r)]r^2 - 0.019k^3 r^3 + [-0.00044k^4 + 0.0029k^4ln(1.07236k) + 0.0029k^4 ln(r)]r^4 + 0.000898k^5r^5 + [0.00012k^6 – 0.000094 k^6ln(1.07236k) - 0.000094 k^6ln(r)] r^6 – 0.000021k^7r^7 + [-3.035×$10^{-6}k^8$ + 1.69×$10^{-6}k^8$ln(1.07236k)+ 1.69×$10^{-6}k^8$ln(r)]r^8 + 2.99×$10^{-7}k^9r^9$ + [4.14×$10^{-8}k^{10}$ – 1.94×$10^{-8}k^{10}$ln(1.07236k) – 1.94×$10^{-8}k^{10}$ln(r)]r^{10} (18)

However this equation (Eq. 18) is not valid when r = 0.

C. System Discretization

Since the displacements of the surface of a half-space are considered equal to the beam deflection (i.e. $y_k=x_k$) the inertia force J_k can be given by Eq.(19)

$$J_i = -M_i \frac{d^2 y_i(t)}{dt^2} = -M_i \frac{d^2 v_i(t)}{dt^2} = M_i \omega^2 \cos(\omega t) v_i \quad (19)$$

$$V_i = \frac{-k}{2\pi G 0} \sum_{j=1}^{n} n X_j F_{ij}$$, here $F_{ij}=I_{21}+I_3$

Taking into account the preceding formulas defining the system parameters (3), the system can now be represented in the following matrix form.

$$[A] \begin{bmatrix} X_1 \\ \vdots \\ X_n \\ \varphi_0 \\ u_0 \end{bmatrix} = \begin{bmatrix} 0 \\ \vdots \\ \vdots \\ \vdots \\ 0 \end{bmatrix} \quad (20)$$

©IJRASET: All Rights are Reserved | SJ Impact Factor 7.538 | ISRA Journal Impact Factor 7.894 |

$$[A] = \begin{bmatrix} A_{11} & \cdots & A_{1n} & \lambda_1 & 1 \\ \vdots & \ddots & \vdots & \vdots & \vdots \\ A_{n1} & \cdots & A_{nn} & \lambda_n & 1 \\ A_{n+1,1} & \cdots & A_{n+1,n} & I_y\omega^2 & 0 \\ A_{n+2,1} & \cdots & A_{n+2,n} & 0 & m\omega^2 \end{bmatrix} \quad (21)$$

Here, Aij denotes the matrix terms obtained through the mathematical transformation after substituting the preceding parameter expressions into system (3).

The beam's Eigenfrequencies are identified by solving the determinant equation of the system matrix (21). To derive the corresponding mode shapes of a beam resting on an inertial half-space, the natural shape associated with each Eigenfrequency must be determined. For this purpose, the unknown X1 in the system is fixed to a unit value, the first equation is removed, and the modified system of n+1 equations with n+1 unknowns is solved. The resulting mode shapes of the beam are then obtained from equation (22).

$$V_i = \frac{-k}{2\pi G0} \sum_{j=1}^{n} X_j F_{ij} \quad ; i=1, 2, 3\ldots n \quad (22)$$

III. ANALYSIS OF BEAM

Material properties used for present analysis are as follows

Shear modulus of soil, $G_0 = 1.125\times10^7 N/m^2$

Poison's ratio, $\nu_0 = 1/3$

Density of soil, $\rho = 2000 kg/m^3$

Young's modulus of beam, $E = 2.1\times10^{10} N/m^2$

Total length of beam, l = 10m

Width of beam, b = 1m

Height of beam, h = 0.5m

Total mass of beam, m = 12500kg

Mass of each section of beam, M_i =1250kg

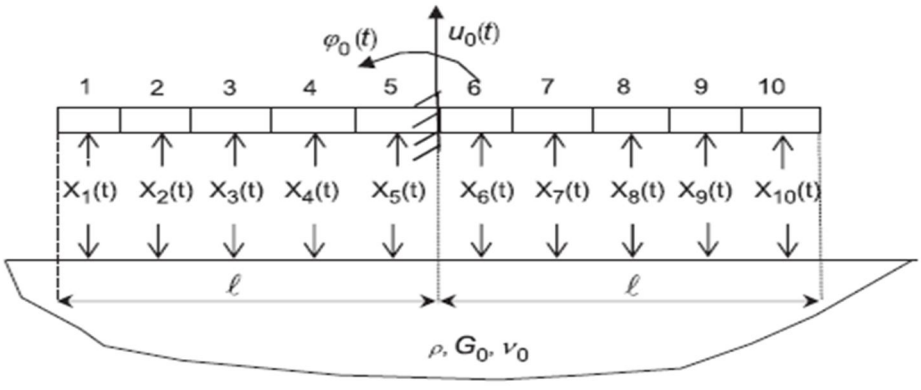


Fig.12. Beam on the surface of an elastic half-space with inertial properties divided into 10 elements

In the present analysis the beam is divided into 10 equal parts and the point f embedment coincides with the centre of mass (Fig.12). Values for the deflections y_{ij} of the beam due to the unit force can be determined by the multiplication of the moment diagrams.

©IJRASET: All Rights are Reserved | SJ Impact Factor 7.538 | ISRA Journal Impact Factor 7.894 |

IV. RESULTS AND DISCUSSIONS

The natural shapes of beam resting on non inertial soil with Discretely Spaced Elastic Supports obtained by NamGyu Park et al. [24] are shown in Fig 13.

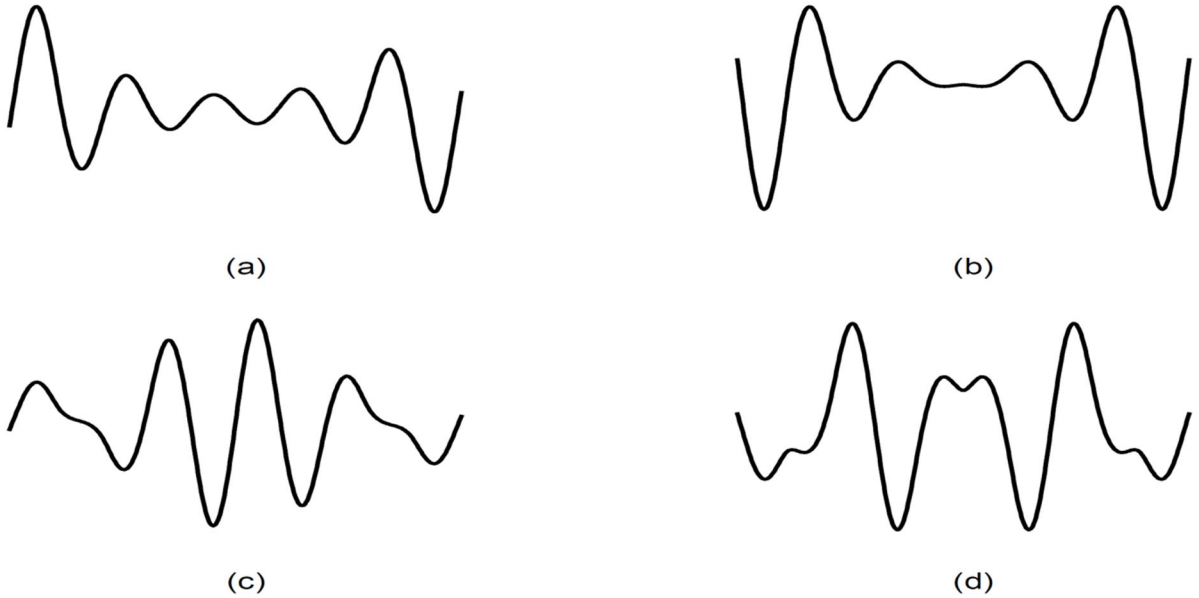


Fig. 13. Irregular natural shape of a beam with discretely placed elastic support (a) First mode (b) Second mode (c) Third mode (d) Fourth mode

The mode shapes of a beam on non inertial soil with continues elastic support obtained by J C O Nielsen [25] is shown in Fig. 14

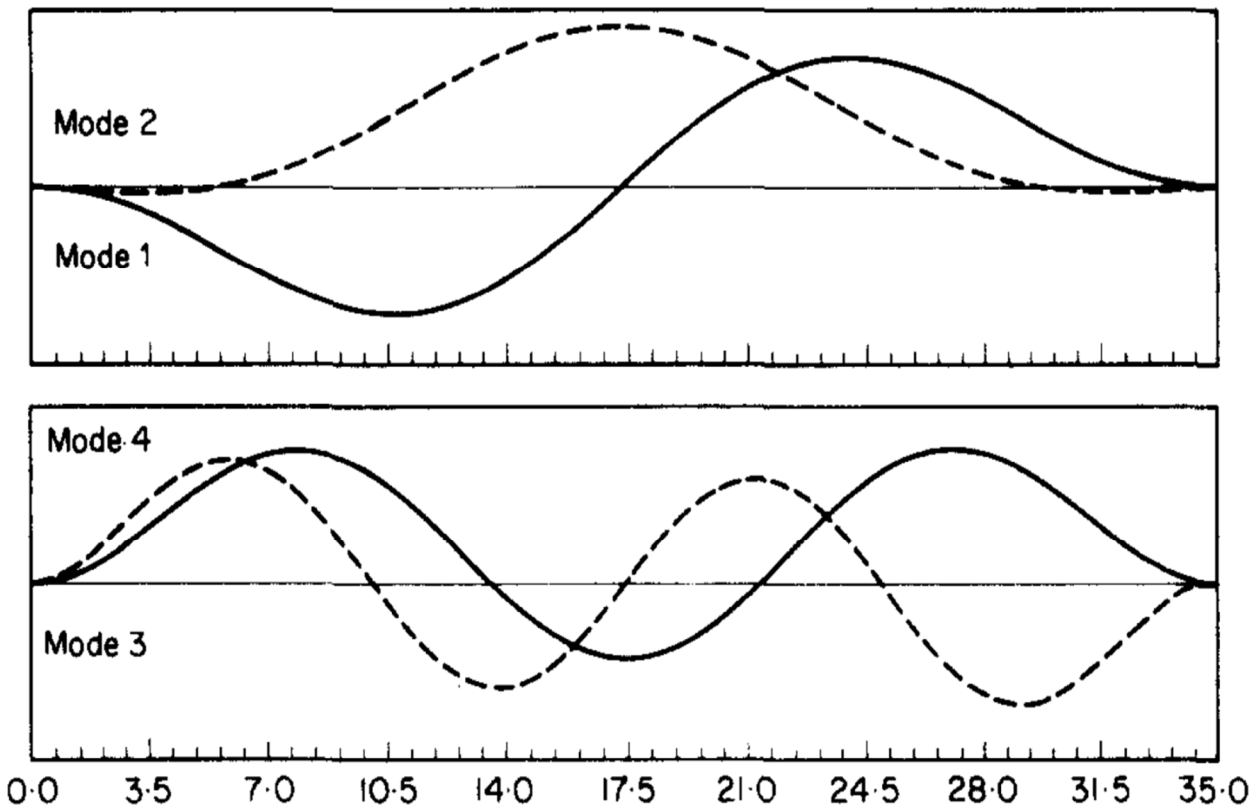


Fig. 14 Mode shapes of beam on elastic foundation

©IJRASET: All Rights are Reserved | SJ Impact Factor 7.538 | ISRA Journal Impact Factor 7.894 |

The values of Eigenfrequencies determined by using I_{21} and I_3 values obtained from integration are,
ω_1 =50, ω_2 =60, ω3 =123.4455, ω4 =150 , ω_5 =216.3, ω_6 =248.92 , ω_7 =300.174
The values of Eigenfrequencies obtained by Guenfoud et.al [3] are,
ω_1 =57.5535, ω_2 =112.7495, ω3 =229.3025, ω_4 =280.8825, ω_5 =291.5572, ω_6 =303.9353
The natural shapes of beam corresponding to each Eigenfrequency obtained are shown in Following figures.

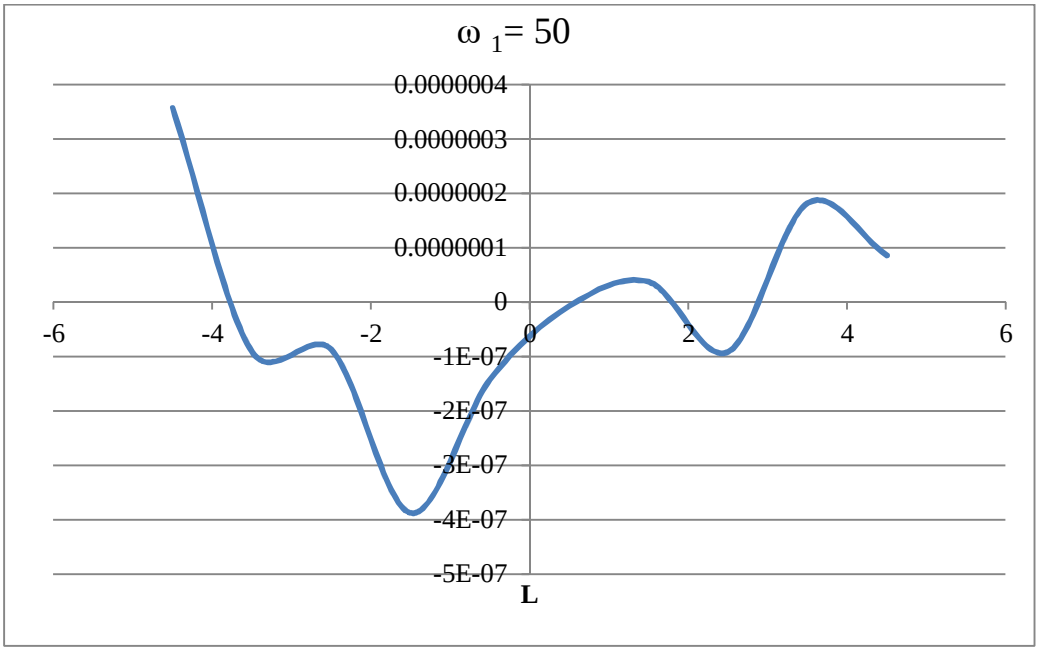


Fig. 15. Natural shape of beam for ω =50

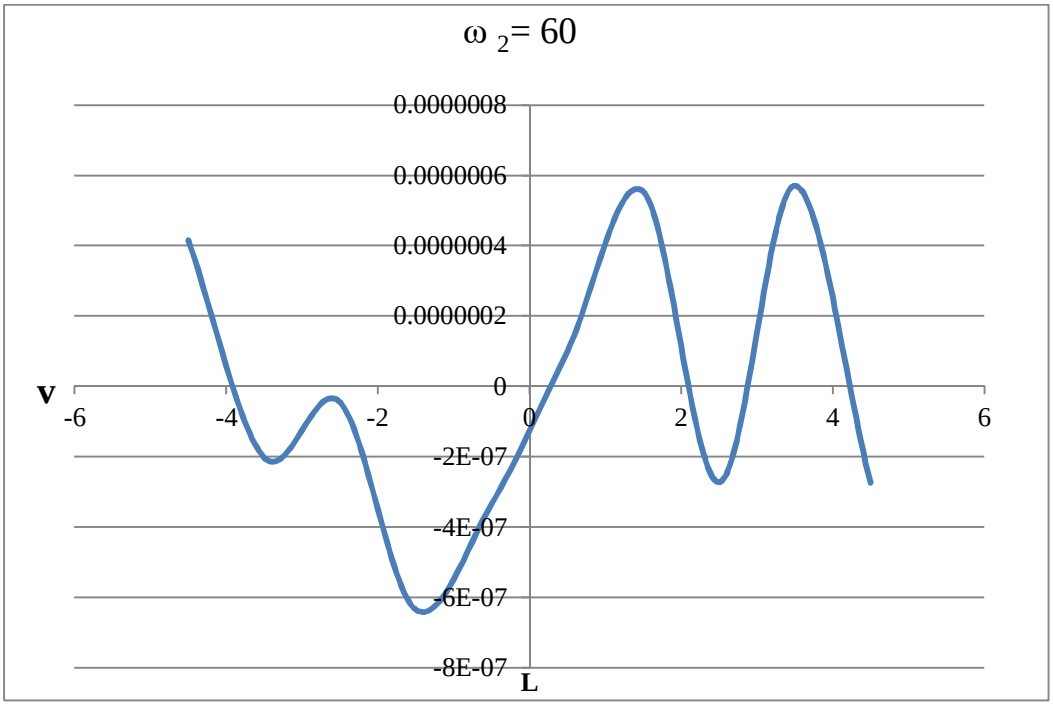


Fig. 16. Natural shape of beam for ω =60

©IJRASET: All Rights are Reserved | SJ Impact Factor 7.538 | ISRA Journal Impact Factor 7.894 |

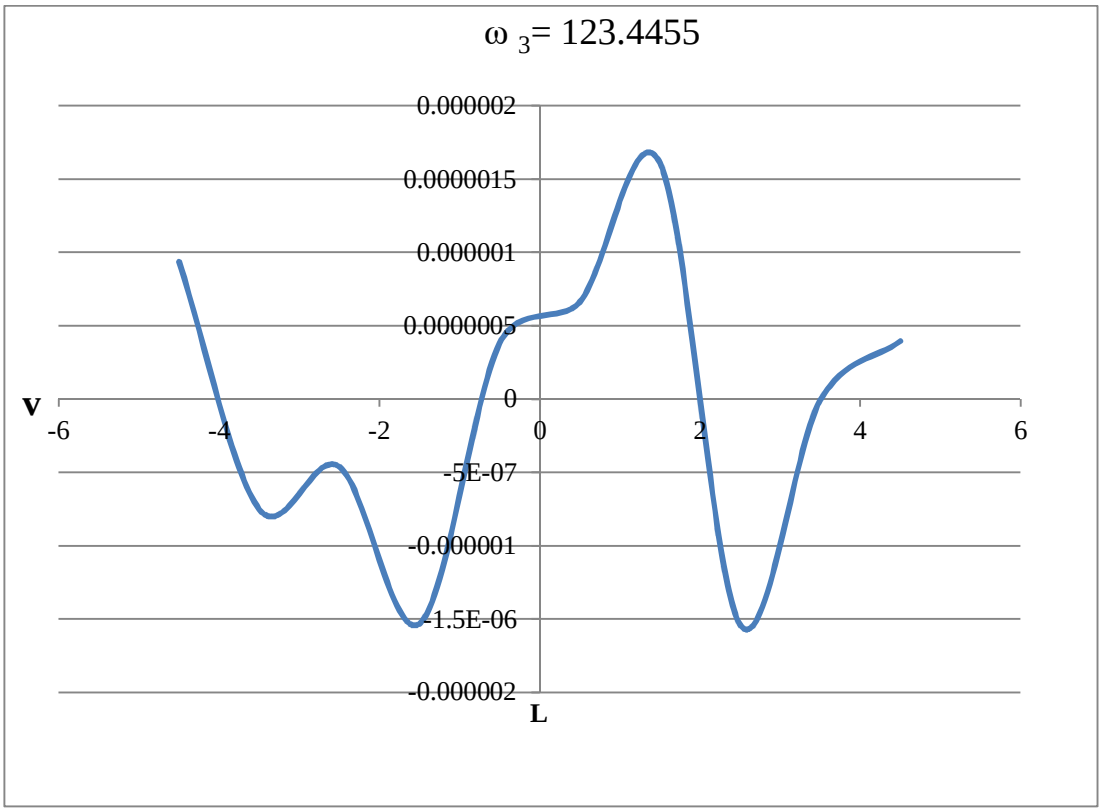


Fig. 17. Natural shape of beam for ω =123.4455

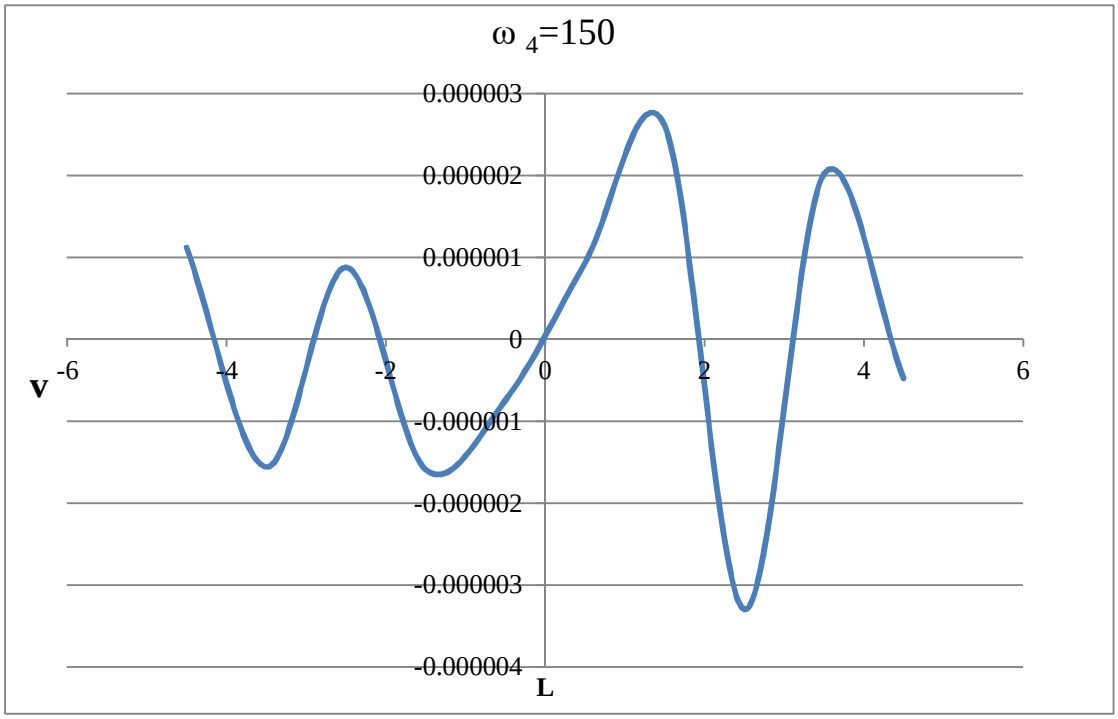


Fig. 18. Natural shape of beam for ω =150

©IJRASET: All Rights are Reserved | SJ Impact Factor 7.538 | ISRA Journal Impact Factor 7.894 |

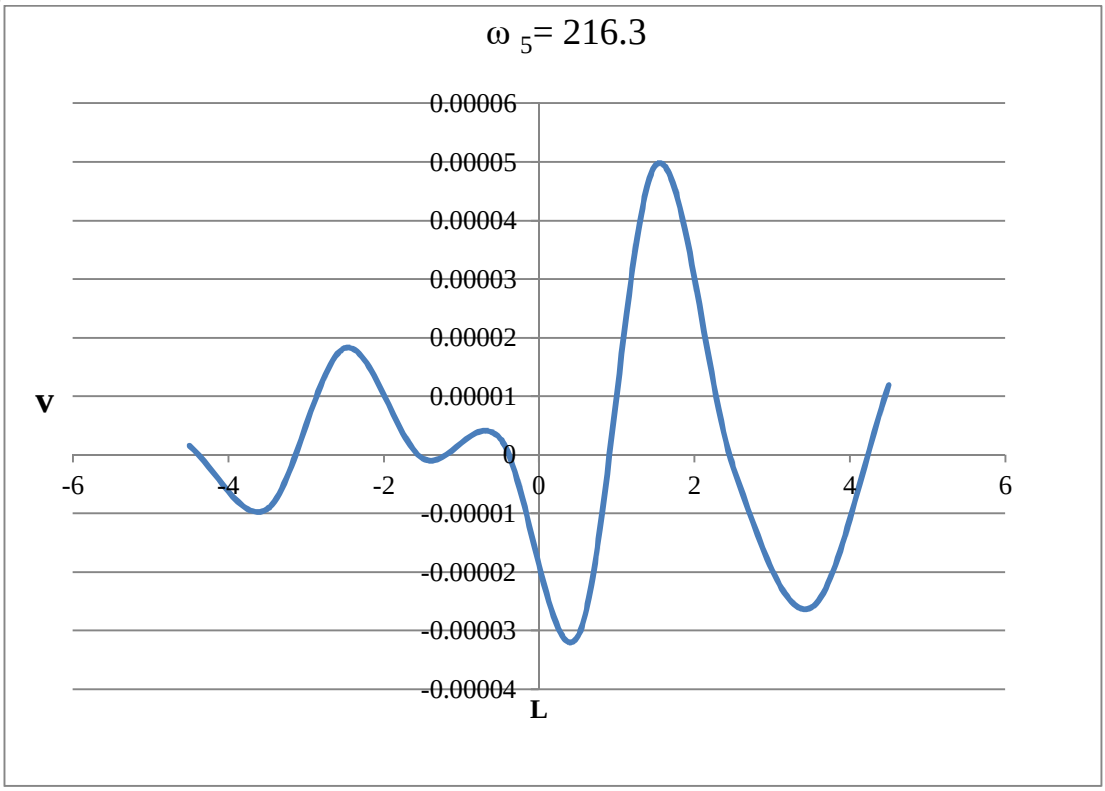


Fig. 19. Natural shape of beam for ω =216.3

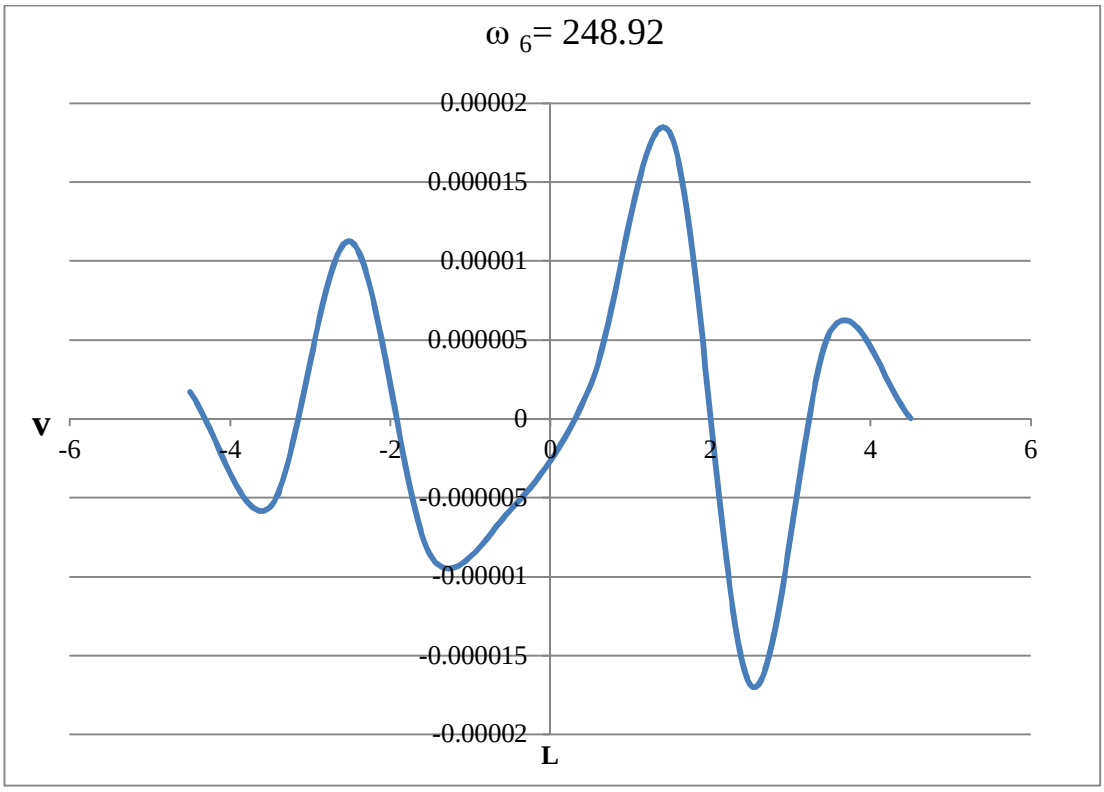


Fig. 20. Natural shape of beam for ω =248.92

©IJRASET: All Rights are Reserved | SJ Impact Factor 7.538 | ISRA Journal Impact Factor 7.894 |

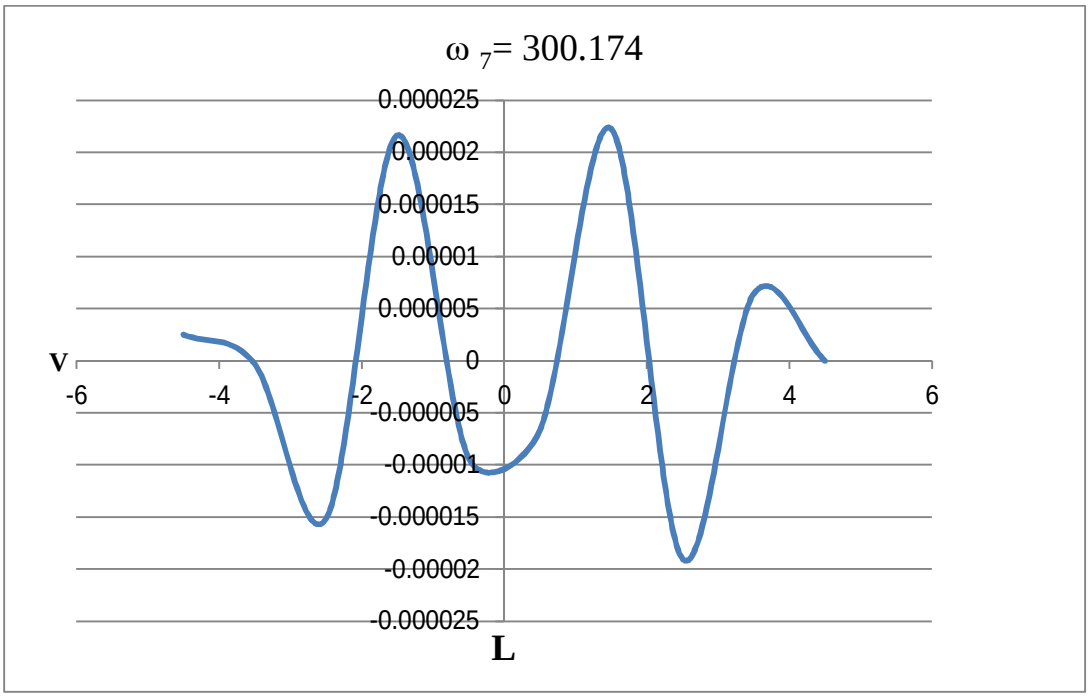


Fig. 21. Natural shape of beam for ω =300.174

The values of Eigenfrequencies obtained by using Eq. (14) are
ω_1 =47.7, ω_2 =60.54 , ω_3 =102.82, ω_4 =141.5, ω_5 =232, ω_6 =304 , ω_7 =350;
The natural shapes corresponding to each Eigenfrequency are shown in Fig. 11.

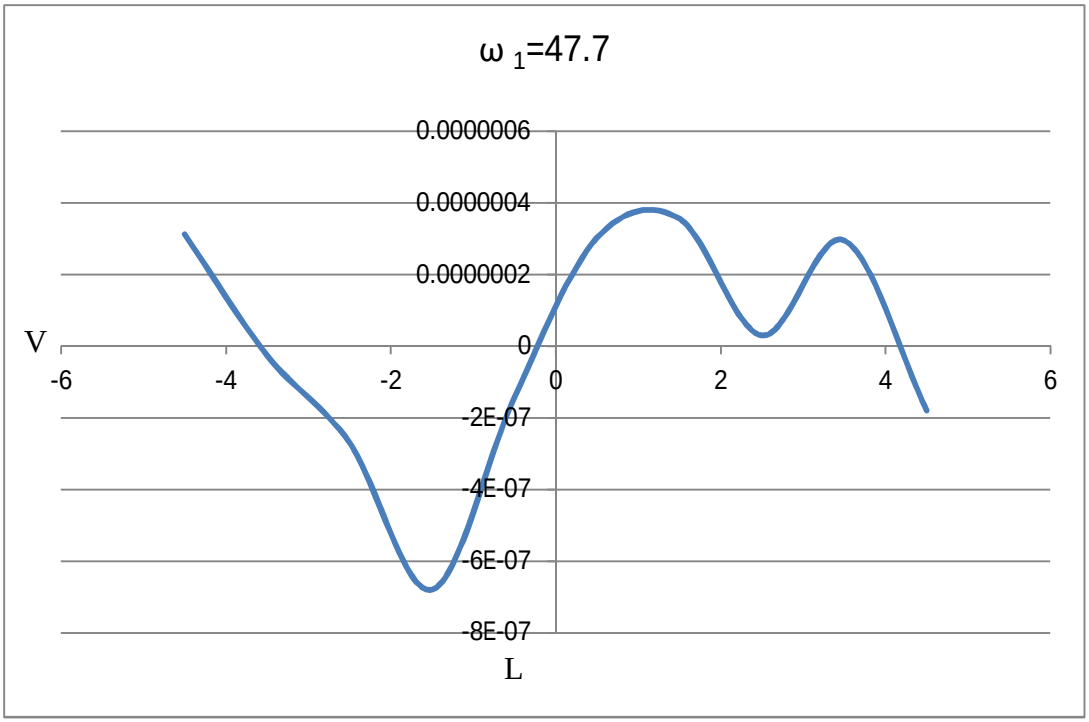


Fig. 22. Natural shape of beam for ω =47.7

©IJRASET: All Rights are Reserved | SJ Impact Factor 7.538 | ISRA Journal Impact Factor 7.894 |

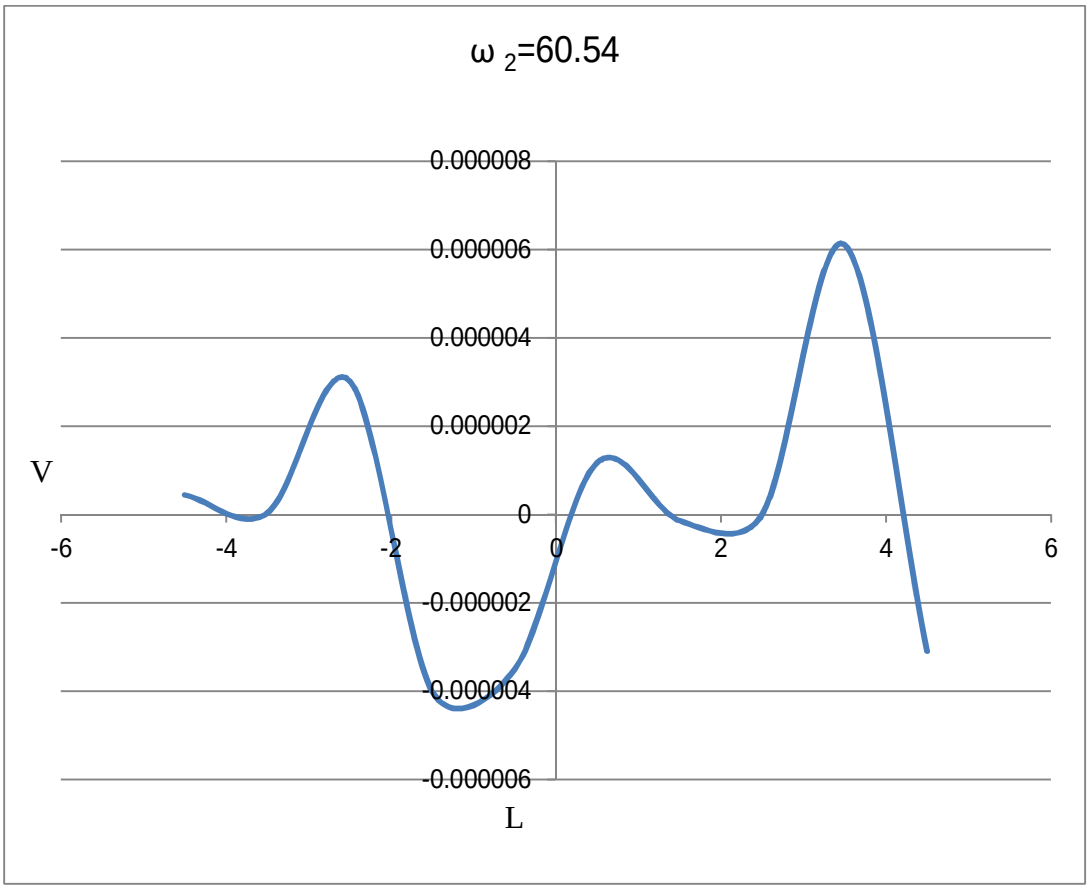


Fig. 23. Natural shape of beam for ω =60.54

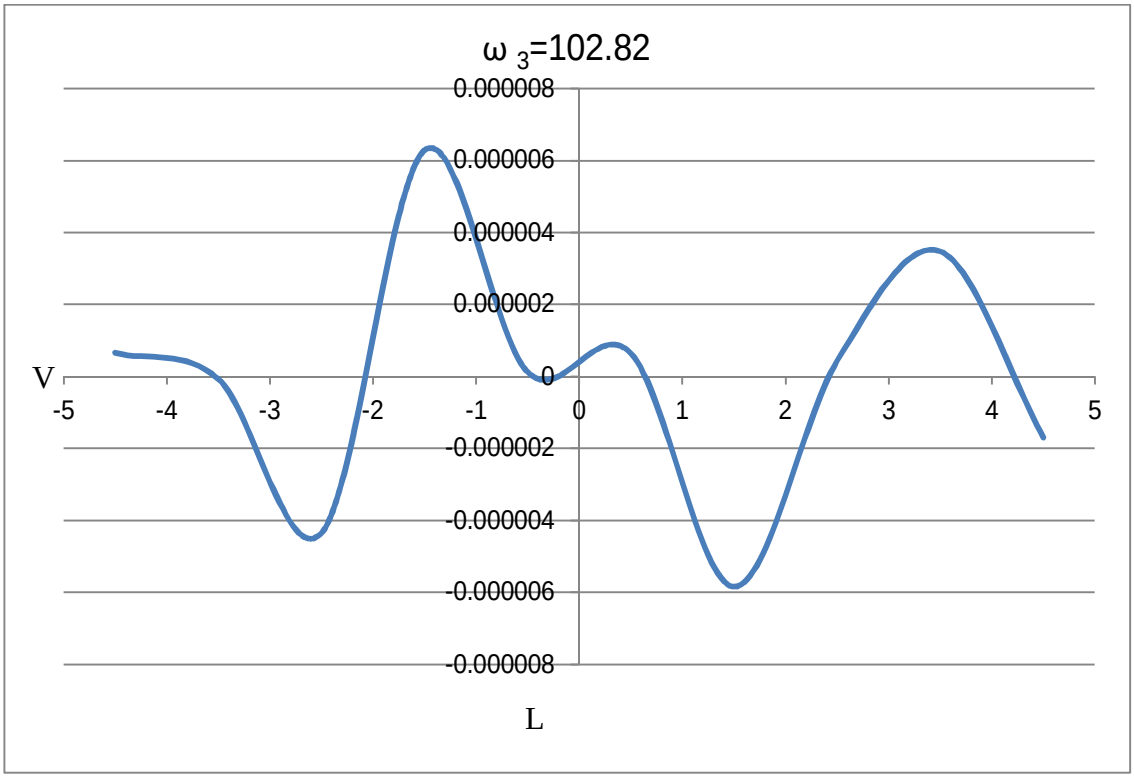


Fig. 24. Natural shape of beam for ω =102.82

©IJRASET: All Rights are Reserved | SJ Impact Factor 7.538 | ISRA Journal Impact Factor 7.894 |

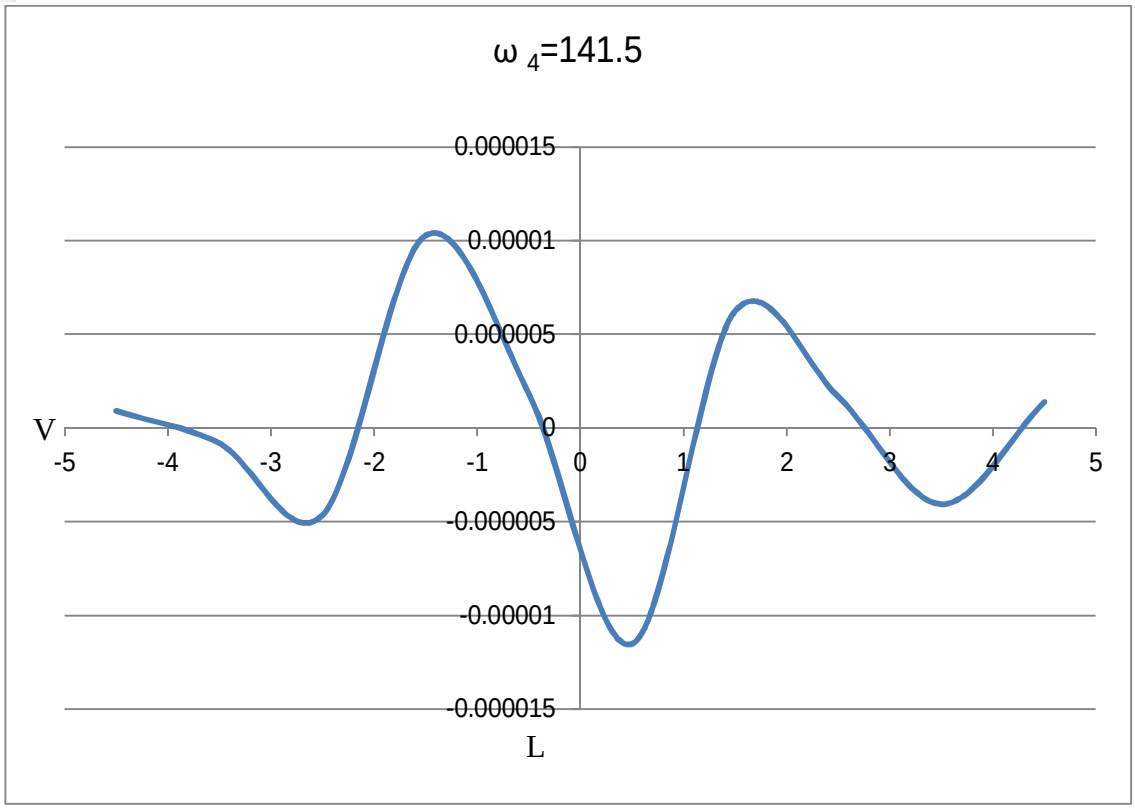


Fig. 25. Natural shape of beam for ω =141.5

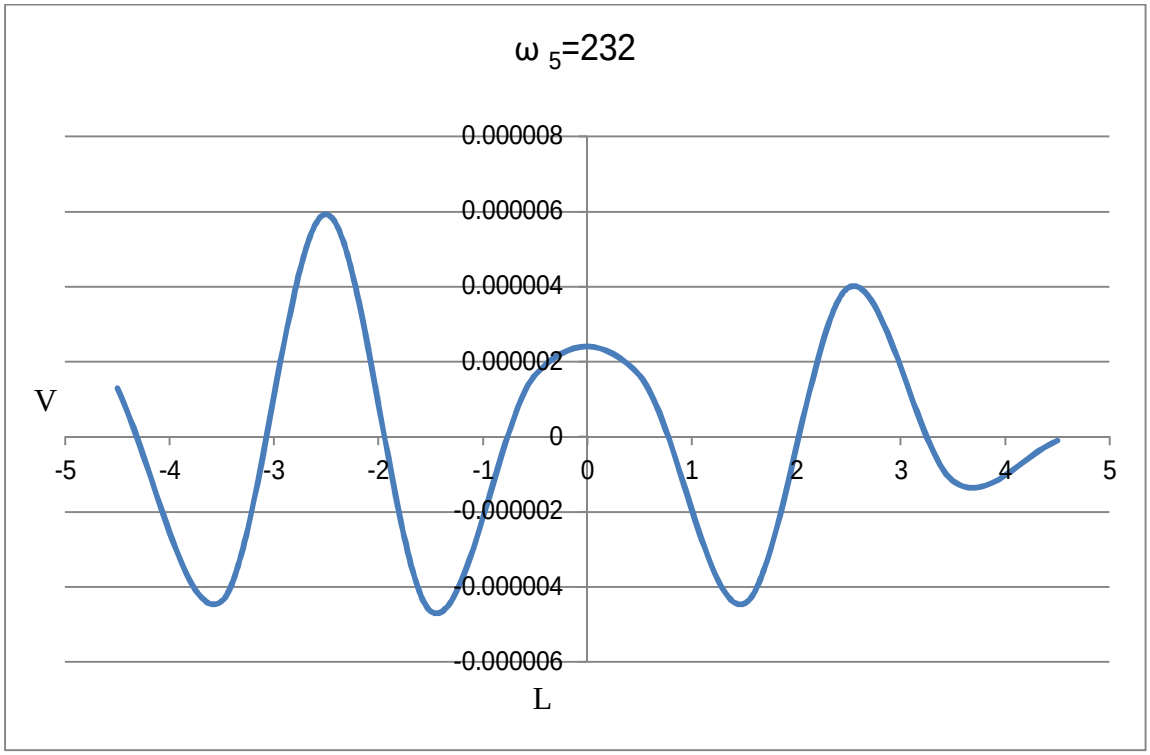


Fig. 26. Natural shape of beam for ω =232

©IJRASET: All Rights are Reserved | SJ Impact Factor 7.538 | ISRA Journal Impact Factor 7.894 |

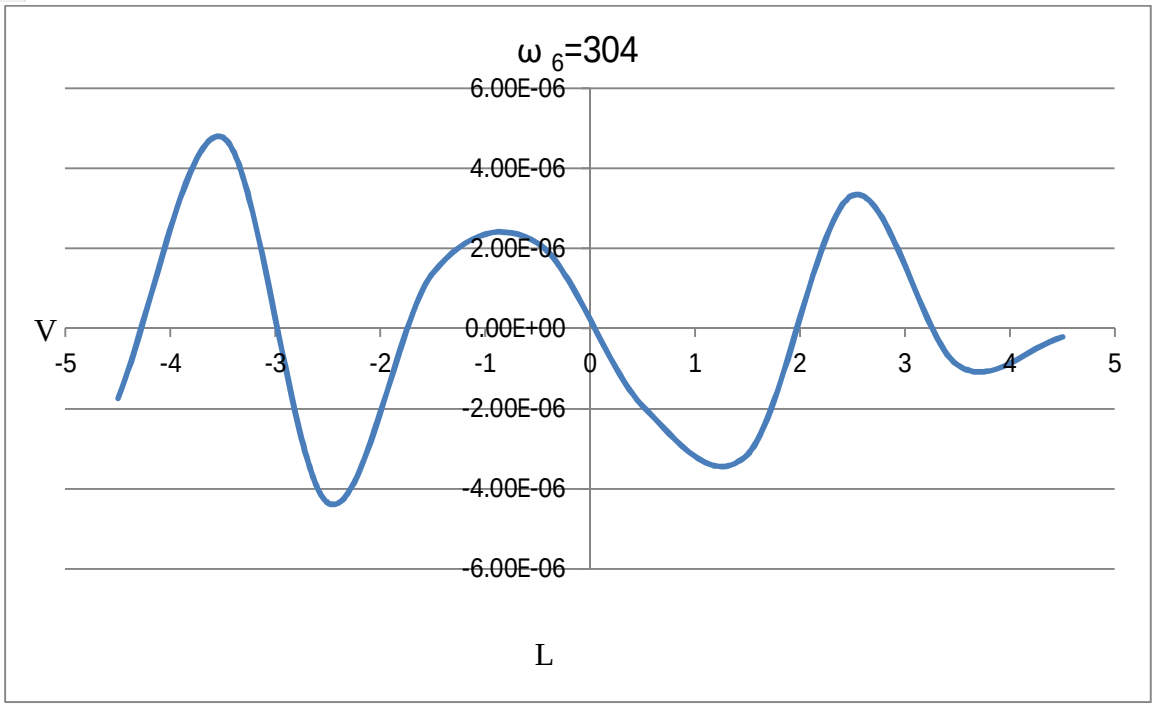


Fig. 27. Natural shape of beam for ω =304

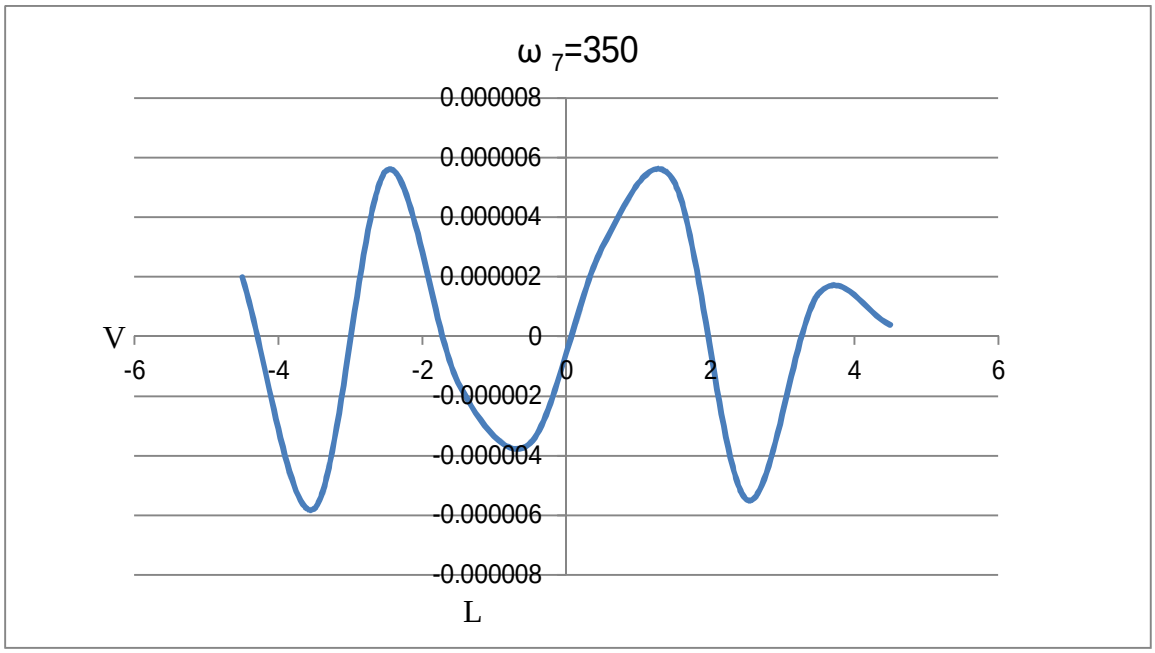


Fig. 28. Natural shape of beam for ω =350

The natural shapes of beam obtained is similar to that obtained for beam resting on non inertial soil with Discretely Spaced Elastic Supports obtained by NamGyu Park et al. [24].

V. CONCLUSION

This paper presents a semi-analytical approach for the dynamic analysis of beams resting on an elastic half-space with inertial properties. The method is developed to evaluate the Eigenfrequencies, mode shapes, and dynamic response of the beam subjected to external excitation.

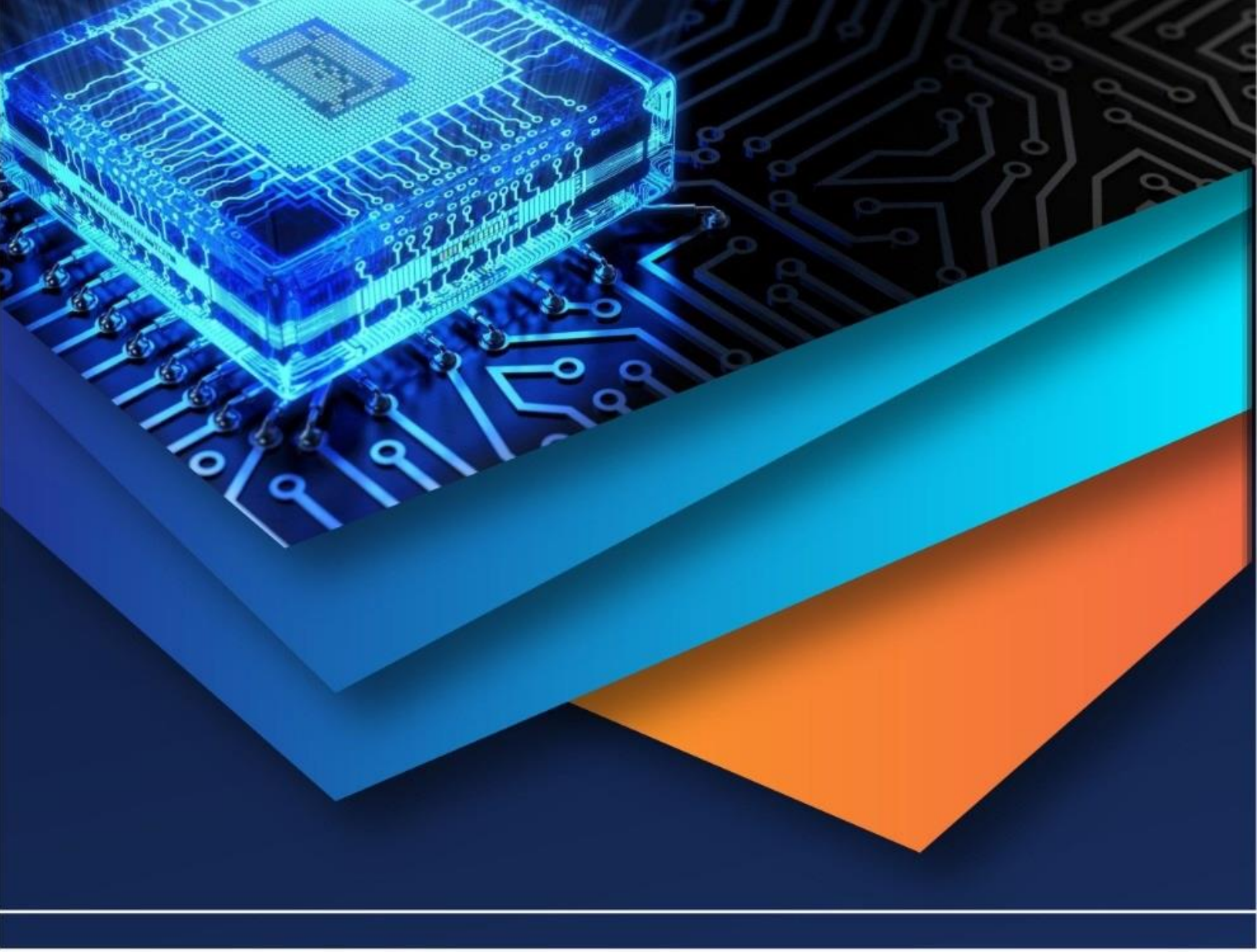
©IJRASET: All Rights are Reserved | SJ Impact Factor 7.538 | ISRA Journal Impact Factor 7.894 |

The analysis considers the interaction forces within the contact zone, which are essential for determining other physical parameters. The formulation is based on Green's functions to represent the displacements in the contact region. Incorporating the inertial effects of the half-space, also known as Lamb's problem, introduces mathematical challenges, particularly due to instabilities associated with hypergeometric functions. The present work overcomes these limitations and provides stable, reliable expressions for the solution. Results show that the computed mode shapes of the beam are irregular, and the proposed semi-analytical method is both computationally efficient and practical for engineering applications. Furthermore, the approach can serve as an approximation function in numerical models, enabling its application to more complex problems of wave propagation and dynamic soil–structure interaction.

REFERENCES

[1] Lamb H. On the propagation of tremors over the surface of an elastic solid. Philosophical Transactions of the Royal Society of London 1904;A 203:1–42.
[2] Graff Karl F. Wave motion in elastic solids. Courier Dover Publications;1991.
[3] Guenfoud S, Amrane MN, Bosakov SV, Ouelaa N. Semi-analytical evaluation of integral forms associated with Lamb's problem. Soil Dynamics and Earth-quake Engineering 2008;29;438-43.
[4] Guenfoud S, Bosakov SV, Laefer DF. Dynamic analysis of a beam resting on an elastic half-space with inertial properties. Soil Dynamics and Earth- quake Engineering 2009; 29; 1198-207
[5] Reissner E. Stationare, axialsymmetrische, druch ein schuttelnde Masse erregte Schwingungeneines homogenen elastische Halbraumes. Ingenieur Archiv 1936; 7(6):381–396.
[6] Shekhter O.Y. The taking into account of the inertial properties of the ground in the calculation of a foundation unit on forced vibration. The work's collection of N.I.I.O., vibration of constructions and foundations 1948;(2):p.72–89;
[7] Bycroft G.N. Forced vibrations of a rigid circular plate on a semi infinite elastic space and on an elastic stratum. Philos Trans R Soc Lond 1956; 248(A.948):327–68.
[8] Pekeris CL. The seismic buried pulse. Proceedings of the National Academy of Sci USA 1955;41:469–80.
[9] Guan F., Novak M. Transient response of an elastic homogeneous halfspace to suddenly applied rectangular loading. Journal of Applied Mechanics: ASME 1994;61:256–263.
[10] Shinozuka M., Deodatis G., Zhang R., Papageorgiou A.S. Modeling, synthetics and engineering applications of strong earthquake wave motion. Soil Dynamics and Earthquake Engineering 1999;18:209–228.
[11] Jin B., Liu H. Exact solution for horizontal displacement at center of the surface of an elastic half space under horizontal impulsive punch loading. Soil Dynamics and Earthquake Engineering 1999;18(7): p.495–498.
[12] Jin B. Elastic halfspace under impulsive, distributed, vertical loading at surface: exact solution at center for a punch-like distribution. Soil Dynamics and Earthquake Engineering 1998;17(5):311–316.
[13] Jin B. Exact solution for horizontal displacement at center of the surface of an elastic halfspace under horizontal impulsive punch loading. Soil Dynamics and Earthquake Engineering 1999;18:495–508.
[14] Zhou X.L., Wang J.H., Lu J.F. Transient foundation solution of saturated soil to impulsive concentrated loading. Soil Dynamics and Earthquake Engineering 2002;22:273–281.
[15] Pradhan P.K., Baidya D.K., Ghosh D.P. Dynamic response of foundations resting on layered soil by cone model. Soil Dynamics and Earthquake Engineering 2004;24:425–434.
[16] Gazetas G. Formulas and charts for impedances of surface and embedded foundations. Journal of Geotechnical Engneering ASCE1991;117(9):1363–81.
[17] Zhemochkin BN, Sinitsyn AP. Practical methods of the calculation of beams and plates resting on an elastic foundation. Moscow: Stroyizdat publishing company; 1962 .
[18] Johnson K. Contact interaction's mechanics. Moscow: Mir publishing company; 1989 (Russian Edition).
[19] Georgiadis HG, Vamvatsikos D, Vardoulakis I. Numerical implementation of the integral-transform solution to Lamb's point-load problem. Comput Mech 1999; 24:90–9.
[20] Zeng S, Liang R. A fundamental solution of a multilayered half-space due to an impulsive ring source. Soil Dyn Earthquake Eng 2002; 22(7):541–50
[21] Zimmermann, H., 1888. The calculation of the railway superstructure. Ernst & Korn, Berlin.
[22] Winkler, E., 1867. The theory of elasticity and strength with special reference to their application in the technology. Dominicus, Prag.
[23] Boussinesq (1885). Potential application of the study of equilibrium and motion of elastic solids.
[24] Nam-Gyu Park, Sang-Youn Jeon, Shin-Ho Lee, Kyeong-Lak Jeon, Joon-Ro Lee, Kyu-Tae Kim Mark. E. Dye. Dynamic Analysis of a Beam with Discretely Spaced Elastic Supports. Journal of Mechanical Science and Technology ; Volume 18 Number 5 (2004), 733-741
[25] J. C. O. Nielsen. Eigenfrequencies and Eigenmodes of a beam structure on an elastic foundation. International Journal for Numerical Methods in Engineering. 1992; 33: 1843-1859

©IJRASET: All Rights are Reserved | SJ Impact Factor 7.538 | ISRA Journal Impact Factor 7.894 |
115



10.22214/IJRASET

45.98

IMPACT FACTOR: 7.129

IMPACT FACTOR: 7.429

INTERNATIONAL JOURNAL FOR RESEARCH

IN APPLIED SCIENCE & ENGINEERING TECHNOLOGY

Call : 08813907089 (24*7 Support on Whatsapp)